ISSN 0036-0244, Russian Journal of Physical Chemistry A, 2023, Vol. 97, No. 2, pp. 367–372. © The Author(s), 2023. This article is an open access publication.
Russian Text © The Author(s), 2023, published in Zhurnal Fizicheskoi Khimii, 2023, Vol. 97, No. 2, pp. 252–257.

PHYSICAL CHEMISTRY OF NANOCLUSTERS, SUPRAMOLECULAR STRUCTURES, AND NANOMATERIALS

Effect of a Geometric Potential on the Eigenfunction and Eigenvalue of the Energy of State in a Twisted Graphene Nanoribbon

N. R. Sadykov[a,*], Yu. A. Petrova[a], I. A. Pilipenko[a], R. S. Khrabrov[a], and S. N. Skryabin[a]

[a]*Snezhinsky Institute of Physics and Technology, National Research Nuclear University MEPhI, Snezhinsk, 456776 Russia*

**e-mail: n.r.sadykov@rambler.ru*

Received May 21, 2022; revised July 11, 2022; accepted July 20, 2022

Abstract—An expression is obtained for an effective geometric potential based on a coordinate system for a nanoribbon twisted in the form of a helicoid. The effective geometric potential for a Schrödinger equation is used to study a graphene nanoribbon of finite length with "armchair" edges under the action of an external electric field parallel to them. Solutions are calculated for the energy levels and wave functions of electrons in the vicinity of the Dirac point. It is shown there is only one state in the transverse direction.

Keywords: geometric potential, twisted nanoribbons, Weingarten equation, kp-type model

DOI: 10.1134/S003602442302022X

INTRODUCTION

Nanostructures that are two-dimensional geometric objects have unique properties which, along with progress in the production of these structures, make it relevant to study the properties of composite media based on them. A unique property of such two-dimensional objects is the quantum effective geometric potential (GP) [1, 2], i.e., the dependence of the potential energy of a system on the purely geometric parameters of its surface. The geometric potential is of quantum origin because it is proportional to the square of Planck's constant $\hbar$. This pattern means that physical effects begin to manifest on a nanometer scale. In real systems with radii of curvature on the order of hundreds of nanometers, the geometric potential is still very small and has an energy scale of less than 1 K, which hinders the experimental realization and exploitation of many phenomenal phenomena [3–9]. Fullerenes and nanotubes are nanoparticles that have 1–10 nm radii of surface curvature. The geometric potential for such nanoparticles can affect their frequency of surface vibrations [10]. The geometric potential caused by the pressure of the flexural excitation of curvature creates an additional normal surface force. For fullerenes and nanotubes, the topicality of studying surface vibrations is due to our meager knowledge of the phenomenon in the region of such small sizes and the centimeter range of emitted wavelengths.

Another nanoparticle for which geometric potential produces phenomenal effects are twisted nanoribbons. The electron transport properties of twisted graphene nanoribbons were studied in [11–17]. A nanoribbon was considered a continuous object in [11], allowing for the experimental results in [12] and ignoring any discreteness of the main hexagonal lattice. Properties of free electrons in the helicoidal geometry of Schrödinger materials were considered in [2, 13, 14]. Results based on the Dirac equation for a confined quantum particle on a submanifold in R3 were presented in works [15–18].

With nanotubes, the geometric potential can affect the nature of the motion of charge carriers. Such a problem is relevant in chiral spintronics [19–23]. Intense studies of the properties of nanotubes based on silicene and germanene are now under way. Silicene (SiNT) nanotubes were synthesized [24] in 2001, and a number of SiNT growth processes have been reported since then. It has been proposed that SiNT be used to create field-effect transistors, waveguides, optoelectronic elements, replacements for graphite in lithium-ion batteries, and heterojunctions that are combinations of carbon and silicon nanotubes [25–28]. The effect of a geometric potential will manifest in the nonaxisymmetric motion of particles in nanotubes, which is equivalent to a projection of the orbital momentum of charge carriers onto the axis of the nanotube. This leads in turn to the elimination of spin degeneracy in nanotubes, due to spin–orbit interaction [23].

In this work, we study the effect geometric potential has on the electron transport properties of twisted graphene armchair nanoribbons in a longitudinal electric field. In analogy with [12, 29], we use a kp-type continuum model.

GEOMETRIC POTENTIAL OF FREE ELECTRONS ON A HELICOID

Let us obtain the dependence of the potential energy of the system on purely geometric parameters in the case of a helicoid. To do so, we use results from [2, 10].

We begin with a three-dimensional curvilinear coordinate system in the form

$$\mathbf{R}(q^1, q^2, q^3) = \mathbf{r}(q^1, q^2) + q^3\hat{\mathbf{N}}(q^1, q^2), \quad (1)$$

where q^1, q^2, q^3 are the contravariant coordinates of a 3D coordinate system, $\mathbf{r}(q^1, q^2)$defines the points of a 2D surface, and $\hat{\mathbf{N}}(q^1, q^2)$ is a unit normal to the surface at the considered point [10]. Introducing three-dimensional system (1) using unit normal $\hat{\mathbf{N}}(q^1, q^2)$ allows us to use the Weingarten equation in [30]. Since a two-dimensional surface is uniquely defined in coordinates q^1 and q^2, there is a two-dimensional coordinate system with basis vectors $\mathbf{e}_1$, $\mathbf{e}_2$ and metric tensor $g_{\alpha\beta}$ of dimension 2 (the first quadratic form):

$$\mathbf{e}_\alpha = \partial\mathbf{r}/\partial q^\alpha, \quad \mathbf{e}_\beta = \partial\mathbf{r}/\partial q^\beta, \quad g_{\alpha\beta} = \mathbf{e}_\alpha\mathbf{e}_\beta, \quad (2)$$

where $\alpha, \beta = 1, 2$. Expressions for basis vectors $\boldsymbol{\varepsilon}_1$, $\boldsymbol{\varepsilon}_2$ and metric tensors G_{ij} of dimension 3 follow analogously for a three-dimensional coordinate system:

$$\boldsymbol{\varepsilon}_i = \partial\mathbf{R}/\partial q^i, \quad \boldsymbol{\varepsilon}_j = \partial\mathbf{R}/\partial q^j, \quad G_{ij} = \boldsymbol{\varepsilon}_i\boldsymbol{\varepsilon}_j, \quad (3)$$

where $i, j = 1, 2, 3$.

For convenience in our mathematical calculations, we assume below that (1) contains both two- and three-dimensional curvilinear coordinate systems for the contravariant components of the radius vector:

$$q^1 = u, \quad q^2 = v, \quad q^3 = \xi. \quad (4)$$

An exception is when we need to transition to the covariant components of the radius vector.

According to [2, 10], allowing for the parameters of a two-dimensional surface yields the expression for the geometric potential:

$$V_S = -\frac{\hbar^2}{8m_e}\left[\frac{1}{f^2}\left(\frac{\partial f}{\partial\xi}\right)^2 - \frac{2}{f}\frac{\partial^2 f}{\partial(\xi)^2}\right]\Bigg|_{\xi=0}$$
$$= -\frac{\hbar^2}{8m_e}[(\lambda_1+\lambda_2)^2 - 4\lambda_1\lambda_2] = -\frac{\hbar^2}{8m_e}(\lambda_1-\lambda_2)^2, \quad (5)$$

where the values of the principal curvatures λ_1, $\lambda_2$of the surface are the solution to the equation [30, 31]

$$\begin{vmatrix} b_{11}-\lambda g_{11} & b_{12}-\lambda g_{12} \\ b_{21}-\lambda g_{21} & b_{22}-\lambda g_{22} \end{vmatrix} = 0. \quad (6)$$

In (6), the metric tensor of the two-dimensional surface $g_{\alpha\beta}$ and $b_{\alpha\beta}$ are the first and second quadratic forms, respectively; $f = \sqrt{G/g}$; $dS = \sqrt{g}dudv$ is the elementary area of a two-dimensional surface; $dV = \sqrt{G}dudvd\xi^3$ is the elementary volume; and G and g are the determinants of metric tensors G_{ij} and $g_{\alpha\beta}$.

QUANTUM STATE FOR FREE ELECTRONS ON A HELICOIDAL SURFACE, ALLOWING FOR AN EFFECTIVE GEOMETRIC POTENTIAL BASED ON A TWO-DIMENSIONAL SCHRÖDINGER EQUATION

We now study a helicoidal surface to get an idea of the interaction between quantum particles and curvature for a twisted nanoribbon, and the possible physical effects resulting from it (the structure of a twisted graphene nanoribbon with chair-like edges is shown in Fig. 1). The electron transport properties of twisted graphene nanoribbons were studied in [11–17]. Following da Costa [2], we obtain effective geometric potential (5) of a two-dimensional Schrödinger equation. In analogy with [32] and using the notations in (4), we first introduce the helicoidal coordinate system

$$x^1 = u\cos(\kappa v) + \xi\sin(\kappa v),$$
$$x^2 = u\sin(\kappa v) - \xi\cos(\kappa v), \quad x^3 = v + \kappa u\xi, \quad (7)$$

where x^1, x^2, and $x^3$are Cartesian coordinates; u, v, ξ are helicoidal coordinates; coordinate x^3 is directed along the nanoribbon; and $\kappa = 2\pi/L$, where L is the length of the twist. Based on the familiar relation between basis vectors and coordinates [30], we write the basis vectors for our helicoidal coordinate system:

$$\tilde{\mathbf{e}}_1 = \partial\mathbf{r}/\partial u = (\cos(\kappa v), \sin(\kappa v), \kappa\xi),$$
$$\tilde{\mathbf{e}}_2 = \partial\mathbf{r}/\partial v = \big(\kappa[-u\sin(\kappa v) + \xi\cos(\kappa v)],$$
$$\kappa[u\cos(\kappa v) + \xi\sin(\kappa v)],\ 1\big), \quad (8)$$
$$\tilde{\mathbf{e}}_3 = \partial\mathbf{r}/\partial\xi = (\sin(\kappa v), -\cos(\kappa v), \kappa u).$$

The expression for metric tensor $\tilde{g}_{ij} = \tilde{\mathbf{e}}_i\tilde{\mathbf{e}}_j$ of a helicoidal system of coordinates follows from Eq. (8):

$$\tilde{g}_{ij} = \begin{pmatrix} 1+\kappa^2\xi^2 & 2\kappa\xi & \kappa^2\xi u \\ 2\kappa\xi & 1+\kappa^2[u^2+\xi^2] & 0 \\ \kappa^2\xi u & 0 & 1+\kappa^2u^2 \end{pmatrix}, \quad (9)$$

where $\tilde{g} = \det\tilde{g}_{ij} = [1+\kappa^2u^2]^2$ when $\xi = 0$. It follows from Eq. (9) that helicoidal coordinate system (7) is orthogonal when $\xi = 0$.

Helicoidal coordinate system (7) allows us to write the equation for surface $\mathbf{r}(u, v)$ of a twisted nanoribbon whose edges are spirals around axis of symmetry x^3.

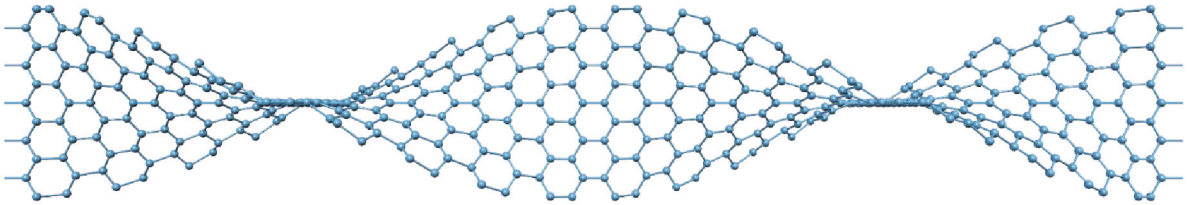

Fig. 1. A helicoidally twisted nanoribbon.

Surface $\mathbf{r}(u,v)$ is a helicoid that with the notation in [2] is described by the equation from (1) for $q^3 = 0$, or is described by coordinate system (7) when $\xi = 0$:

$$\mathbf{r}(u,v) = (x^1, x^2, x^3) = \big(u\cos[\kappa v],\ u\sin[\kappa v],\ v\big). \quad (10)$$

It follows from (8) and (9) that there is a connection between basis vector $\tilde{\mathbf{e}}_3$ of coordinate system (7) and normal $\hat{\mathbf{N}}$ from (1) to the helicoid:

$$\hat{\mathbf{N}} = \frac{1}{[1+(\kappa u)^2]^{1/2}}\tilde{\mathbf{e}}_3\big|_{\xi=0} = \frac{1}{[1+(\kappa u)^2]^{1/2}}\big(\sin(\kappa v),\ -\cos(\kappa v),\ \kappa u\big). \quad (11)$$

To move from coordinate system (7) to coordinate system (1) while allowing for (10), we must assume $dq^3 = h_3 d\xi$, where $h_3 = (1+(\kappa u)^2)^{1/2}$ is the Lame coefficient [33] of the coordinate system (9).

When $\xi = 0$, a two-dimensional helicoidal coordinate system with metric tensor $g_{\alpha\beta}$ (the first quadratic form) and the second quadratic form $b_{\alpha\beta}$ [30] follows from (9):

$$g_{\alpha\beta} = \frac{\partial\mathbf{r}}{\partial q^\alpha}\frac{\partial\mathbf{r}}{\partial q^\beta} = \begin{pmatrix} 1 & 0 \\ 0 & 1+(\kappa u)^2 \end{pmatrix},$$
$$b_{\alpha\beta} = \hat{\mathbf{N}}\frac{\partial^2\mathbf{r}}{\partial q^\alpha \partial q^\beta}\bigg|_{q^2=0} = \begin{pmatrix} 0 & \dfrac{-\kappa}{[1+(\kappa q^1)^2]^{1/2}} \\ \dfrac{-\kappa}{[1+(\kappa u)^2]^{1/2}} & 0 \end{pmatrix}. \quad (12)$$

From (6) and (11) we obtain expressions for the values of main curvatures λ_1, λ_2:

$$\lambda_1 = -\lambda_2 = \kappa/[1+(\kappa u)^2]. \quad (13)$$

This leads to the expression for the geometric potential,

$$V_S = -\frac{\hbar^2}{8m_e}(\lambda_1 - \lambda_2)^2 = -\frac{\hbar^2}{2m_e}\frac{\kappa^2}{[1+(\kappa u)^2]^2}. \quad (14)$$

It follows from the expression for the potential that the eigenvalue of the energy of an isolated state will be a negative value.

Based on first quadratic form $g_{\alpha\beta}$ from equalities (12) for Schrödinger materials [2, 13, 14], and considering expression (14) for the geometric potential, we obtain the equation for a particle for the wave function, allowing for longitudinal electric field W:

$$\left[\frac{\partial^2}{\partial(u)^2} + \frac{\kappa^2 u}{1+(\kappa u)^2}\frac{\partial}{\partial u} + \frac{\kappa^2}{[1+(\kappa u)^2]^2}\right]\Psi + \frac{1}{[1+(\kappa u)^2]}\frac{\partial^2\Psi}{\partial(v)^2} = -\frac{2m_e}{\hbar^2}(E + |e|Wv)\Psi. \quad (15)$$

In this work, we consider narrow armchair-edge nanoribbons with staggered configuration N-AGNRs, where $N = 11$ [29, 34, 35]. With $m = (N-1)/2 = 5$, nanoribbon width $H = m\sqrt{3}b \approx 1.23$ nm, where $b = 0.142$ nm is the distance between the carbon atoms in graphene. With length $L = 10H$ of the period of a helicoidal nanoribbon, it follows that $[1+(\kappa q^1_{\max})^2] \approx 1.05$, where $q^1_{\max} = H/2$, $\kappa L = 2\pi$. Under condition $\kappa q^1_{\max} \ll 1$ for a solitary nanoribbon, we can obtain an approximate solution to Eq. (15) via the separation of variables:

$$\Psi = \Phi_1(u)\Phi_2(v),$$
$$\frac{\partial^2}{\partial v^2}\Phi_2 = -\frac{2m_e}{\hbar^2}(E - E_1 + |e|Wv)\Phi_2, \quad (16)$$
$$\left[\frac{\partial^2}{\partial(u)^2} + \frac{\kappa^2 u}{1+(\kappa u)^2}\frac{\partial}{\partial q^1} + \frac{\kappa^2}{[1+(\kappa u)^2]^2}\right]\Phi_1 = -\frac{2m_e}{\hbar^2}E_1\Phi_1$$

with boundary conditions $\Phi_2(v = \pm L/2) = 0$, $\partial\Phi_1(u = \pm H/2)/\partial u = 0$, where L and H are the length and width of the nanoribbon, and E and E_1 are constant energies. If necessary, the accuracy of calculations can be refined by means of perturbation theory [36].

The solution to function Φ_2 of the first equation in (16) is expressed in terms of Airy functions $Ai(\zeta)$ and $Bi(\zeta)$ [36, 37]:

$$\Phi_2(\zeta) = C_1 Ai(\zeta) + C_2 Bi(\zeta), \quad (17)$$

where C_1 and C_2 are constant values,

$$\zeta = (2m_e|e|W/\hbar^2)^{1/3}[q^2 + (E - E_1)/|e|W],$$

$$\left[\frac{2m_e|e|W}{\hbar^2}\right]^{1/3}\left[-\frac{L}{2}+\frac{(E-E_1)}{|e|W}\right]\le\zeta$$
$$\le\left[\frac{2m_e|e|W}{\hbar^2}\right]^{\frac{1}{3}}\left[\frac{L}{2}+\frac{(E-E_1)}{|e|W}\right],\quad \frac{\partial^2}{\partial\zeta^2}\Phi_2=-\zeta\Phi_2.$$

Let us find the solution to the second equation in (16). We introduce new variable $\varsigma=\tanh(\sqrt{2}\kappa u)$ and, based on the condition $(\kappa u)^2\ll 1$ for the nanoribbon, we transform the second Schrödinger equation from (16) into

$$\frac{\partial^2\Phi_1}{\partial\varsigma^2}-\frac{3\varsigma}{2(1-\varsigma^2)}\frac{\partial\Phi_1}{\partial\varsigma}+\frac{m_eE_1/(\hbar\kappa)^2+(1-\varsigma^2)/2}{(1-\varsigma^2)^2}\Phi_1=0, \tag{18}$$

where $V_S=-\hbar^2\kappa^2(1-\varsigma^2)/(2m_e)$, $\cosh(\sqrt{2}\kappa q^1)\approx 1+(\kappa u)^2$.

Equation (18) is a generalized hypergeometric equation [37]:

$$\frac{\partial^2\Phi_1}{\partial\varsigma^2}+\frac{\tilde{\tau}}{\sigma}\frac{\partial\Phi_1}{\partial\varsigma}+\frac{\tilde{\sigma}}{\sigma^2}\Phi_1=0, \tag{19}$$

where $\sigma=1-\varsigma^2$, $\tilde{\tau}=-3\varsigma/2$, and $\tilde{\sigma}=(1-\varsigma^2)/2+m_eE_1/(\hbar\kappa)^2$. Generalized hypergeometric Eq. (19) is easily reduced to

$$(1-\varsigma^2)\frac{\partial^2y}{\partial\varsigma^2}+\left(-2\varsigma-\varsigma\sqrt{\frac{1}{4}-\frac{4m_eE_1}{(\hbar\kappa)^2}}\right)\frac{\partial y}{\partial\varsigma}$$
$$+\left(\frac{m_eE_1}{(\hbar\kappa)^2}+\frac{1}{4}-\frac{1}{2}\sqrt{\frac{1}{4}-\frac{4m_eE_1}{(\hbar\kappa)^2}}\right)y=0, \tag{20}$$

where

$$\Phi_1=y(\varsigma)\varphi(\varsigma),\quad \varphi=C(1-\varsigma^2)^{\left(\frac{1}{8}+\frac{1}{4}\sqrt{\frac{1}{4}-\frac{4m_eE_1}{(\hbar\kappa)^2}}\right)}. \tag{21}$$

RESULTS AND DISCUSSION

A series of calculations was performed for narrow armchair-edge nanoribbons of staggered configuration [29, 34, 35]. In calculations for the armchair-edge nanoribbons with staggered configuration N-AGNRs, where $N=11$, it was assumed that $m=(N-1)/2=5$, nanoribbon width $H=5\sqrt{3}b\approx 1.23$ nm, $b=0.142$ nm, helicoidal nanoribbon period $L=10H$, $-H/2\le q^1_{\max}\le H/2$, and $\kappa L=2\pi$. It should be noted that graphene nanoribbons with 7-AGNR armchair edges of a symmetrical configuration with width $H=3\sqrt{3}b$ have now been synthesized, based on the technology of vapor deposition.

It follows from our calculated results that there is only one stationary state $|n=1\rangle$ in the transverse direction when the second boundary condition $\partial\Phi_1(u=\pm H/2)/\partial u=0$, the energy level of which is $E_{1,n=1}=0.3(V_S)_{\max}=-\dfrac{0.3\hbar^2\kappa^2}{2m_e}=-3\times10^{-3}$ eV, is satisfied. Due to narrow width H of the nanoribbon, there is no stationary state $|n=1\rangle$ when the first boundary condition $\Phi_1(u=\pm H/2)u=0$ is satisfied. When there is no torsion and the first boundary condition is satisfied at nanoribbon boundary $\Phi_1(u=\pm H/2)=0$, energy level $|E_1|\sim 2\pi^2\hbar^2/(mH^2)\approx 1$ eV follows from (16). This is much higher than energy $E_{1,n=1}=0.3(V_S)_{\max}=-3\times10^{-3}$ eV of stationary state $|n=1\rangle$ when the second boundary condition is satisfied at the edge of the nanoribbon. Figure 2 shows the dependence of the square on the modulus of eigenfunction $|\Phi_1(\varsigma)|^2$ (curve *1*) of main states $E_{1,n=1}$ of ς, where $\varsigma=\tanh(\sqrt{2}\kappa u)$ and u is a transverse coordinate. Figure 2 shows the dependence of hypergeometric function $y(z)$ on variable z, where $z=(1-\varsigma)/2$. Two solutions to the hypergeometric Eq. (20) were defined inside circle $|z|<1$ of hypergeometric series [36, 37]

$$y_1=F(\alpha,\beta,\gamma,z)=1+\frac{\alpha\beta}{\gamma}\frac{z}{1!}$$
$$+\frac{\alpha(\alpha+1)\beta(\beta+1)}{\gamma(\gamma+1)}\frac{z^2}{2!}+\ldots, \tag{22}$$

$$y_2=z^{1-\gamma}F(\beta-\gamma+1,\ \alpha-\gamma+1,\ 2-\gamma,z). \tag{23}$$

Dashed curve *2* corresponds to first solution y_1 from (22) of the hypergeometric Eq. (20); solid curve *3* corresponds to second solution y_2 from (23).

CONCLUSIONS

We calculated geometric potential (14) on a helicoidal surface whose maximum value was on the order of $\max|V_S|=\hbar^2\kappa^2/(2m_e)=10^{-2}$ eV at helicoid period $L=12.3$ nm and nanoribbon width $H=0.1L$, where $\kappa=2\pi/L$. It was shown analytically that the principal curvatures of the helicoidal surface were equal in absolute value and opposite in sign. This means the value of the geometric potential was much larger than that of a deformed spherical perturbed surface [10]. With a narrow ribbon, the problem can be solved via the separation of variables, and there is a single isolated state in the transverse direction. The energy level of an isolated state was negative: $E_{n=1}=0.3(V_S)_{\max}=-3\times10^{-3}$ eV when $L=12.3$ nm.

Using a two- and four-point unit cell based on a kp-type continuum model, it was shown in [29] that energy levels form an equidistant spectrum when there

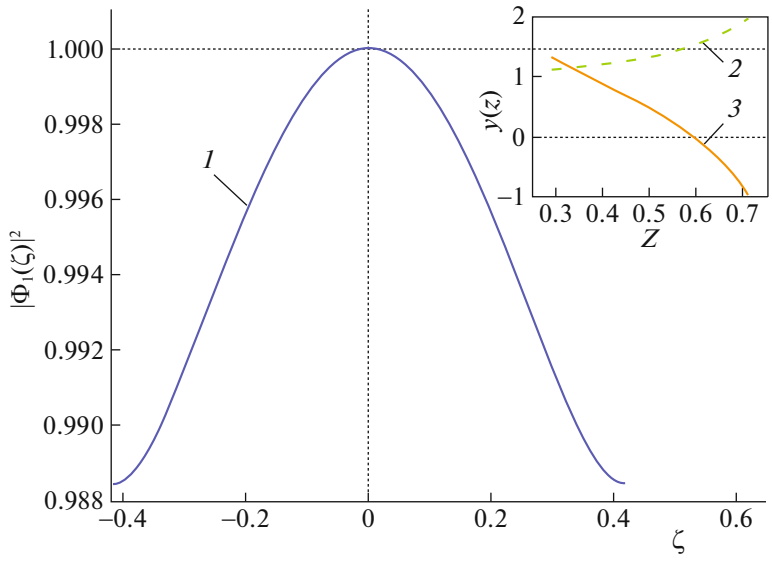

Fig. 2. Dependence of eigenfunction $|\Phi_1(z)|^2$ of ground state $E_{1,n=0} = -3\times10^{-3}$ eV on z.

is a longitudinal stationary electric field in carbon nanotubes and narrow flat nanoribbons:

$$E_{1,k} = E_1 + \varepsilon_k, \quad \varepsilon_k = [\pi\hbar v_F/(2L_0)](1+2k), \quad (24)$$

where $k = 0, \pm1, \pm2, \pm3, \pm4$; $v_F = 3b|\tau|/(2\hbar)$ is the Fermi velocity; $\tau = -|\tau|$, where τ is the integral of the transition; $\hbar$ is Planck's constant; and L_0 is the length of the nanoribbon. When $L_0 = 50$ nm, the difference between adjacent equidistant energy levels $\Delta\varepsilon = \varepsilon_k - \varepsilon_{k-1}$ from (24) is $\Delta\varepsilon = \dfrac{\pi\hbar v_F}{L_0} \approx 2\times10^{-2}$ eV. Such results follow when the Dirac (Majorana) equation is used instead of Schrödinger's. The evolution of isospin is then described by Hermite's equation [38], while the evolution of charge carriers is described using the Airy functions (17) in accordance with (16). This problem is outside the scope of this work.

The results obtained in this work are of great interest when charge carriers move in nanotubes along helicoidal trajectories. The authors of [23] studied the formation of spin minigaps caused by the torsional deformation of nonchiral hexagonal armchairs (n, n) and zigzag (n, 0) silicon nanotubes (SiNT). In this work, spin degeneracy in nanotubes (the Rashba effect) was eliminated via spin–orbit interaction.

FUNDING

The authors thank National Research Nuclear University MEPhI for their support under the Project 5-100 Competitiveness Enhancement Program, contract no. 02.a03.21.0005.27.08.2013.

OPEN ACCESS

REFERENCES

1. H. Jensen and H. Koppe, Ann. Phys. **63**, 586 (1971). https://doi.org/10.1016/0003-4916(71)90031-5
2. R. S. T. Costa, Phys. Rev. A **23**, 1982 (1981). https://doi.org/10.1103/PhysRevA.23.1982
3. G. Cantele, D. Ninno, and G. Iadonisi, Phys. Rev. B **61**, 3730 (2000). https://doi.org/10.1103/PhysRevB.61.13730
4. H. Aoki, M. Koshino, D. Takeda, et al., Phys. Rev. B **65**, 035102 (2001). https://doi.org/10.1103/PhysRevB.65.035102
5. M. Encinosa and L. Mott, Phys. Rev. A **68**, 014102 (2003). https://doi.org/10.1103/PhysRevA.68.014102
6. J. Gravesen and M. Willatzen, Phys. Rev. A **72**, 032108 (2005). https://doi.org/10.1103/PhysRevA.72.032108

7. A. Marchi, S. Reggiani, M. Rudan, and A. Bertoni, Phys. Rev. B **72**, 035403 (2005). https://doi.org/10.1103/PhysRevB.72.035403
8. A. I. Vedernikov and A. V. Chaplik, J. Exp. Theor. Phys. **90**, 397 (2000).
9. C. Ortix and J. van den Brink, Phys. Rev. B **81**, 165419 (2010). https://doi.org/10.1103/PhysRevB.81.165419
10. N. R. Sadykov and N. V. Yudina, Tech. Phys. **65**, 369 (2020). https://doi.org/10.1134/S1063784220030226
11. V. Atanasov and A. Saxena, Phys. Rev. B **92**, 035440 (2015). https://doi.org/10.1103/PhysRevB.92.035440
12. N. Mohanty, D. Moore, Z. Xu, et al., Nat. Commun. **3**, 844 (2012). https://doi.org/10.1038/ncomms1834
13. R. Dandoloff and T. T. Truong, Phys. Lett. A **325**, 233 (2004). https://doi.org/10.1016/j.physleta.2004.03.050
14. V. Atanasov, R. Dandoloff, and A. Saxena, Phys. Rev. B **79**, 033404 (2009). https://doi.org/10.1103/PhysRevB.79.033404
15. M. Burgess and B. Jensen, Phys. Rev. A **48**, 1861 (1993). https://doi.org/10.1103/PhysRevA.48.1861
16. V. Atanasov and A. Saxena, Phys. Rev. B **81**, 205409 (2010). https://doi.org/10.1103/PhysRevB.81.205409
17. Y. N. Joglekar and A. Saxena, Phys. Rev. B **80**, 153405 (2009). https://doi.org/10.1103/PhysRevB.80.153405
18. V. Atanasov and A. Saxena, J. Phys.: Condens. Matter **23**, 175301 (2011).
19. S. H. Yang, Appl. Phys. Lett. **116**, 120502 (2020).
20. S. H. Yang, R. Naaman, Y. Paltiel, and S. S. P. Parkin, Nat. Rev. Phys. **3**, 328 (2021).
21. K. Michaeli, N. Kantor-Uriel, R. Naamanm, and D. H. Waldeck, Chem. Soc. Rev. **45**, 6478 (2016).
22. R. Naaman and D. H. Waldeck, Ann. Rev. Phys. Chem. **66**, 263 (2015).
23. P. N. D'yachkova and E. P. D'yachkov, Appl. Phys. Lett. **120**, 173101 (2022). https://doi.org/10.1063/5.008690
24. I. Kiricsi, A. Fudala, Konya, et al., Appl. Catal. A **203**, 1 (2000).
25. M. de Crescenzi, P. Castrucci, M. Scarselli, et al., Appl. Phys. Lett. **86**, 231901 (2005).
26. A. Morata, M. Pacios, G. Gadea, et al., Nat. Commun. **9**, 4759 (2018).
27. H. Wu, G. Chan, and J. W. Choi, Nat. Nanotechnol. **7**, 310 (2012).
28. C. K. Chan, H. Peng, G. Liu, et al., Nat. Nanotechnol. **3**, 31 (2008).
29. N. R. Sadykov, E. T. Muratov, I. A. Pilipenko, and A. V. Aporoski, Phys. E (Amsterdam, Neth.) **120**, 114071 (2020). https://doi.org/10.1016/j.physe.2020.114071
30. B. A. Dubrovin, S. P. Novikov, and A. T. Fomenko, *Modern Geometry: Methods and Applications,* 2nd ed. (Fizmatlit, Moscow, 1986) [in Russian].
31. M. A. Spivak, *Comprehensive Introduction to Differential Geometry* (Publ. or Perish, Boston, 1999).
32. N. R. Sadykov, Quantum Electron. **26**, 271 (1996).
33. B. M. Budak, A. A. Samarskii, and A. N. Tikhonov, *Collection of Problems on Mathematical Physics,* 4th ed. (Fizmatlit, Moscow, 2004) [in Russian].
34. A. Onipko and L. Malysheva, Phys. Status Solidi **255**, 1700248 (2017). https://doi.org/10.1002/pssb.201700248
35. R. W. Boyd, *Nonlinear Optics* (Academic, San Diego, 2003).
36. L. D. Landau and E. M. Lifshitz, *Course of Theoretical Physics,* Vol. 3: Quantum Mechanics: Non-Relativistic Theory, 4th ed. (Oxford Univ. Press, Oxford, 1980; Nauka, Moscow, 1989).
37. A. F. Nikiforov and V. B. Uvarov, *Special Functions of Mathematical Physics* (Fizmatlit, Moscow, 1978) [in Russian].
38. N. R. Sadykov, Theor. Math. Phys. **180**, 1073 (2014). https://doi.org/10.1007/s11232-014-0200-z

Translated by M. Drozdova